Study of the structure and dynamics of ionic liquids using Pulsed Field Gradient(PFG)-NMR Spectroscopy

Riyaz Ahmed

A dissertation submitted for the partial fulfilment of BS-MS dual degree in Science

Indian Institute of Science Education and Research Mohali
April 2019

Certificate of Examination

This is to certify that the dissertation titled **Study of the structure and dynamics of ionic liquids using pulsed field gradient(PFG)-NMR Spectroscopy** submitted by **Riyaz Ahmed** (Reg. No. MS14050) for the partial fulfillment of BS-MS dual degree programme of the Institute, has been examined by the thesis committee duly appointed by the Institute. The committee finds the work done by the candidate satisfactory and recommends that the report be accepted.

Dr. Arvind | Dr. Kamal P. singh | Dr. Kavita Dorai (Supervisor)

Dated: April 25, 2019

Declaration

The work presented in this dissertation has been carried out by me under the guidance of Prof. Kavita Dorai at the Indian Institute of Science Education and Research Mohali, India.

This work has not been submitted in part or in full for a degree, a diploma, or a fellowship to any other university or institute. Whenever contributions of others are involved, every effort is made to indicate this clearly, with due acknowledgement of collaborative research and discussions. This thesis is a bonafide record of original work done by me and all sources listed within have been detailed in the bibliography.

Riyaz Ahmed
(Candidate)

Dated: April 25, 2019

In my capacity as the supervisor of the candidates project work, I certify that the above statements by the candidate are true to the best of my knowledge.

Dr. Kavita Dorai
(Supervisor)

Acknowledgment

I would like to thank my supervisor, Prof. Kavita Dorai for their scientific and moral support that made this thesis so enjoyable.
I would like to acknowledge Prof. Arvind and Dr. Kamal P. singh for being my committee member.
Special thanks to Ms. Jyotsna Ojha for helping in sample preparation and doing experiments on spectrometer. I am thankful to Ms. Mamta Bhandari for helping in handling glove box and sample preparation. I am thankful to Amandeep Singh, Sumit Mishra, Rakesh Sharma, Dileep Singh, Akshay Gaikwad, Akansha Gautam for being supportive lab members.
My sincere thanks to my friends Pardeep Tanwar, Misbah, Ajeet Dheeman, Nitin Burman, Jaideep Mali.
Last but not the least my parents and siblings for bearing me during the ups and downs.
I want to dedicate my thesis to my parents and elder brother Rizwan Ahmad.

List of Figures

Abstract

Nuclear Magnetic Resonance (NMR) spectroscopy is a versatile technique that has contributed a lot in determining the structure of almost any organic and biological molecule. Another important function of NMR spectroscopy is that it provides highly accurate kinetic data for complex liquid system. The application of NMR spectroscopy to ionic liquids has significantly grown in recent years. Here, NMR spectroscopy is exploited to do translational motion study of ionic liquids.

Ionic liquids possess various outstanding properties such as low vapor pressure, nonflammable and thermal and chemical stability[2], but have low ionic conductivity. Since Ionic liquids are used as a dielectric medium in various devices such as lithium-ion batteries, however, due to poor ionic conductivity, their energy storage capacity is low. Here we proposed a method to see the effect on ionic conductivity after mixing two ionic liquids from measured diffusion coefficient using Pulsed field gradient (PFG)-NMR and Relaxation NMR. Further, the study of the effect of ionic liquids on insulin fibril formation and also study of the change in the behavior of ionic liquid in a confined environment such as inside carbon nanotube will be studied.

Contents

Chapter 1

Introduction

1.1 Motivation

In the present world, there are various catastrophic and irreversible events such as rising of sea levels, acidification of oceans, polar melts, droughts, flood and global warning occurring because of continuous rise in CO_2 level in the atmosphere [24]. In this context, the efficient electrical energy storage devices are very much required to keep control of CO_2 emission into the atmosphere. Ionic liquids (ILs) are used as electrolytes in various electrical energy storage devices such as lithium battery, supercapacitor and many more. IL possess various outstanding properties such as low vapor pressure, nonflammable and thermal and chemical stability [2], but have low ionic conductivity. Because of this, there energy storage capacity is low. The motivation for me is to enhance the energy storage capacity of these devices by increasing the ionic conductivity after mixing ionic liquids. Two more things strengthen my motivation to work with ILs. First is to study the effect of ionic liquids on insulin fibril formation and second is to see the change in the behavior of ionic liquids inside a confined environment.

1.2 NMR Spectroscopy

Spectroscopy can be defined as the study of the interaction of light with matter. It is the fundamental exploratory tool in the field of science, allow to investigate the composition and structure of matter at the molecular scale, micro scale and over astronomical distance. In particular, NMR is a technique that relies on the intrinsic spin properties of nuclei. In which spins are first exposed to a strong and constant

magnetic field. Then, they are excited by a radio frequency pulse sequence. The precession of the spins is recorded during the free induction decay of the NMR experiment and converted into a frequency spectrum after Fourier transformation.

1.2.1 Nuclear spin and the splitting of energy levels in magnetic field

Nuclear spin is the fundamental property just like an electric charge. It can be understood as a form of angular momentum, but it is not produced by rotation of particles whereas it is an intrinsic property of particle itself. In many atoms (such as 12C) these spins are paired against each other, such that the nucleus of the atom has no overall spin. However, in some atoms (such as 1H and 13C) the nucleus does possess an overall spin [1]. Each elementary particle is characterized by nuclear spin angular momentum quantum number (I). Quantum mechanics tells us that a nucleus of spin I will have 2I + 1 possible orientations. A nucleus with spin 1/2 will have two possible orientations. In the absence of an external magnetic field, these orientations are of equal energy. If a magnetic field is applied, then the energy levels split that is known as **Zeeman splitting**. Each level is given a magnetic quantum number, m.

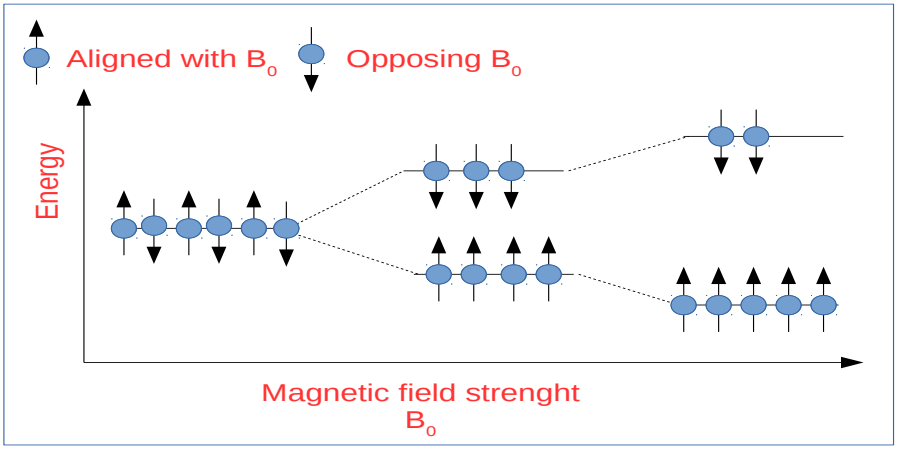

Figure 1.1: Energy levels for a nucleus with spin quantum no 1/2.

When the nucleus is placed in a magnetic field, the initial populations of the energy levels are determined by the Boltzmann distribution that says that the lower energy level will contain slightly more nuclei than the higher level. It is possible to excite these nuclei into a higher level with electromagnetic radiation. The frequency of radiation needed is determined by the difference in energy between the energy levels [1].

The difference in energy between levels (the transition energy) can be found from

$$\Delta E = \gamma \hbar B_0 \tag{1.1}$$

where γ is the gyromagnetic ratio, and B is the applied magnetic field.

Spin as magnetic moment

If we consider a proton, then its spin can be understood in term of a magnetic moment vector. The magnitude of this magnetic moment vector depends on the value of the spin angular momentum which is given by the relation

$$\vec{\mu} = \gamma \hbar \vec{I} \tag{1.2}$$

where μ, γ and I are the magnetic moment, gyromagnetic ratio and spin angular momentum respectively.

1.3 Larmor frequency

When a proton is placed in a magnetic field, it will try to align itself in the direction of the applied magnetic field. The spins either aligned in the direction (lower energy levels) of applied field or in the opposite direction (higher energy levels). As explained by Boltzmann the lower energy level will contain slightly more nuclei than the higher level, That will develop net magnetization along the z-axis (if the applied magnetic field is along the z-axis). If the magnetization is not aligned correctly with the applied magnetic field then this leads to a precessional motion of net magnetization around the z-axis [4, 9]. The angular frequency of this precessional motion is known as **Larmor frequency** and is given by

$$\omega_o = -\gamma B_0 \tag{1.3}$$

where B_0 is the magnitude of applied external magnetic field.

Classical Description

By adopting the analogy from classical mechanics, the interaction energy of a dipole after placing it in an external magnetic field can be written as

$$E_{interaction} = -\vec{\mu}.\vec{B} \tag{1.4}$$

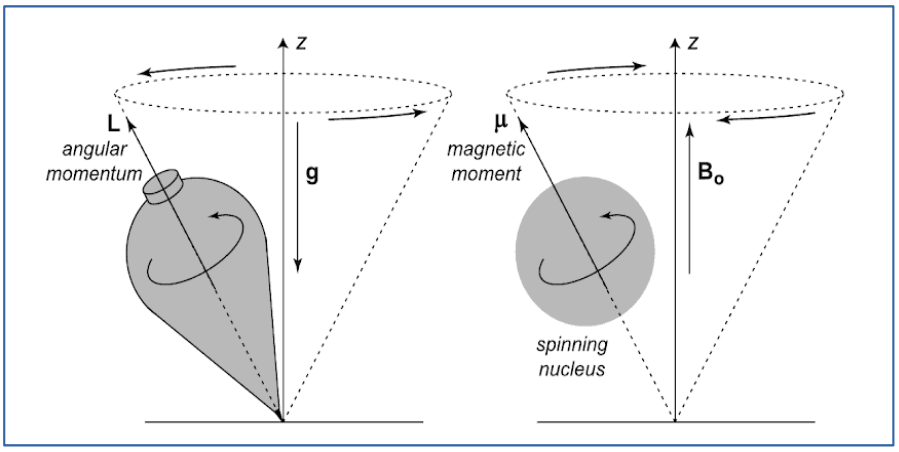

Figure 1.2: Analogy between a spin-top in a gravitational field and magnetic moment in magnetic field [17].

Therefore, by using equation (1.2) and equation (1.3) we can calculate the zeeman hamiltonian when the field is along z-direction.

$$\hat{H}_{zeeman} = -\gamma\hbar\vec{B}\hat{I} = \hbar\omega_o\hat{I}_z \tag{1.5}$$

where $\omega_o = \gamma B_o$ is called the larmor frequency. Therefore, corresponding energies of non-degenerate states are $E_{lower} = -\hbar\omega_o/2$ and $E_{upper} = \hbar\omega_o/2$.

Ensemble Effect

The net magnetization for a sample is the sum of the individual magnetic moments in the sample

$$\vec{M} = \sum_i \vec{\mu_i} \tag{1.6}$$

we have already defined the magnetic moment for a nucleus with spin I in equation (1.2). The magnetization can then be written as

$$\vec{M} = \gamma\vec{J} \tag{1.7}$$

where J is the net spin angular momentum.
The torque, $\vec{\tau}$, of the sample will then be

$$\vec{\tau} = \frac{d\vec{J}}{dt} \tag{1.8}$$

also,

$$\vec{\tau} = \vec{M} \times \vec{B} \tag{1.9}$$

Substituting M for J from equation (1.7) and further solving, equation (1.8) and (1.9) we obtain

$$\frac{d\vec{M}}{dt} = \gamma(\vec{M} \times \vec{B}) \tag{1.10}$$

then

$$\frac{d\vec{M}}{dt} = \gamma MBsin(\theta) \tag{1.11}$$

since $\vec{M}$ and $\vec{B}$ are parallel, the sin term drops out. We want to know the rate at which the magnetization is changing with respect to time, so we take the second derivative and the result is the Larmor frequency

$$\omega_o = \gamma\vec{B} \tag{1.12}$$

since $\vec{M}$ and $\vec{B}$ are both vector quantities, the cross product with B in only the Z direction i.e. ($\vec{B}$=(0, 0, B_0)) then we obtain the Larmor frequency

$$\omega_o = \gamma B_o \tag{1.13}$$

1.4 Magnetisation

At room temperature, the number of spins in the lower energy state are more than that the higher energy states in accordance with the Boltzmann distribution which is given by

$$N_\beta/N_\alpha = exp(-\frac{(E_\beta - E_\alpha)}{k_B T}) \tag{1.14}$$

Where α and β are the energy levels, E_α and E_β are their energies, N_α and N_β are the number of spins in the energy levels respectively, k_B is the Boltzmann constant and T is thermodynamic temperature of the spin system [6].

The difference in the number of the spins in the two energy states leads to the development of a net magnetisation in the sample. This signal in NMR spectroscopy results when transition between these states occur. So NMR can be defined as a physical phenomenon in which nuclei in a magnetic field absorb and re-emit electromagnetic radiation as shown in the figure (1.4). The redistribution of the magnetisation can be done by applying a radio frequency pulse whose frequency matches with the Larmor

frequency of the nuclei [6].

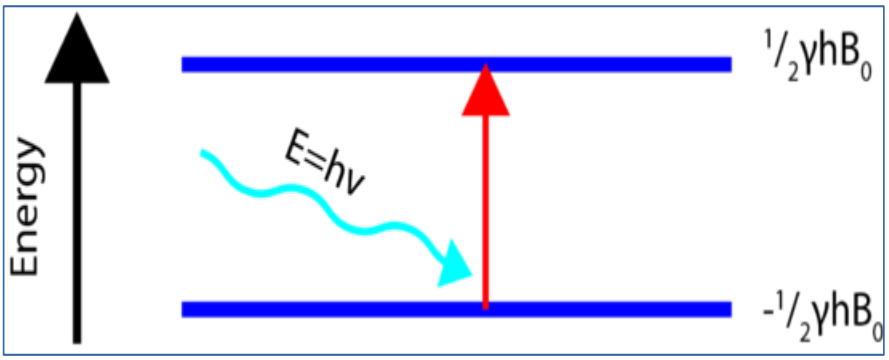

Figure 1.3: Absorption of radiation.

1.5 Chemical shift

The significance of NMR spectroscopy is therefore not based on its ability to differentiate between elements, but on its ability to distinguish a particular nucleus concerning its environment in the molecule. That is, one finds that the resonance frequency of an individual nucleus is influenced by the distribution of electrons in the chemical bond of the molecule [6].
This can be demonstrated using ^1H NMR spectra of methyl acetate. Methyl acetate will produce two different NMR signals, one each for methyl and methoxy as shown in figure (1.5). This effect, produced by the different chemical environment of the protons in the molecule, is known as the chemical shift.
Thus, with an applied magnetic field of 1.4 T, the proton resonances of a molecule do not occur at $\nu_o = 60$ MHz but rather at $\nu \pm \Delta\nu$, where $\Delta\nu$, in general, is less than 1 kHz. Other magnetic nuclei are affected similarly, and this phenomenon forms the basis of applied NMR spectroscopy.

1.6 Spin-Spin interaction

In NMR spectroscopy, there are various types of interaction among the spins or spin and magnetic field. The interaction among the spins could be either through space (called Dipolar coupling) or through bond (called scalar J-coupling).

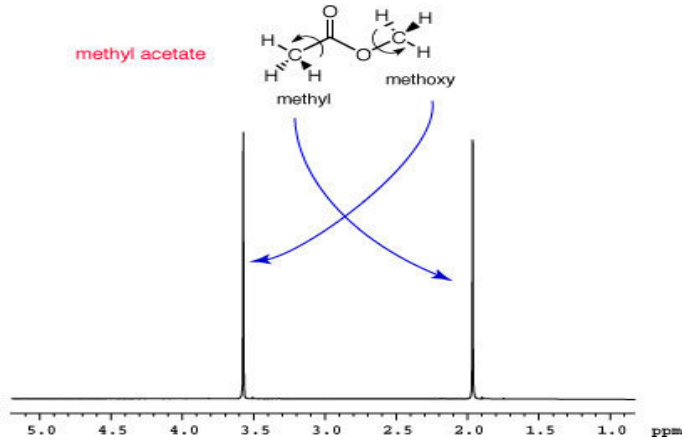

Figure 1.4: The 1H NMR spectra of methyl acetate [16].

Dipolar coupling

The dipole-dipole coupling is the direct magnetic interaction between two close spins. The effect is intra-molecular and inter-molecular since it acts through space. The interaction energy is minimal when the two spins are aligned. This spin interaction is responsible for the Nuclear Overhauser Effect (NOE).

Scalar J-coupling

The scalar J-coupling results from an indirect magnetic interaction of two nuclear spins via their surrounding electrons. The effect is exclusively intra-molecular because it is propagated through the bonds between two nuclei.

1.7 Quantum Mechanical Description of spin placed in static and oscillating field

In elementary quantum mechanics, the Schrodinger equation is given by

$$\iota\hbar\frac{d|\psi\rangle}{dt} = \hat{H(t)}|\psi\rangle \tag{1.15}$$

if $\hat{H}$ is time-independent, then the solution is given by

$$|\psi(t)\rangle = e^{(-\frac{\iota\hat{H}t}{\hbar})}|\psi(0)\rangle \tag{1.16}$$

otherwise, it is given by

$$|\psi(t)\rangle = e^{(\int -\frac{\iota \hat{H(t)} dt}{\hbar})} |\psi(0)\rangle \tag{1.17}$$

Generally, we dealt with the time-dependent Hamiltonian in NMR spectroscopy. In order to simplify the Hamiltonian, we write it in different reference frame so that the time dependency gets cancel out [7]. There are two such frames of references one is interacting frame and other is rotating frame [19].

1.7.1 Interaction frame

The total Hamiltonian of the system could be written as

$$\hat{H}_{total} = \hat{H}_0 + \hat{H}_1 \tag{1.18}$$

Suppose total Hamiltonian of a quantum system comprised of two Hamiltonian with one of the component is too large as compared to other (assume $\hat{H}_0 >> \hat{H}_1$).
To get a better picture of the dynamics of system in presence of $\hat{H}_1$ alone, let us define a new state $|\phi\rangle$.

$$|\phi(t)\rangle = e^{(\frac{\iota \hat{H}_0 t}{\hbar})} |\psi(t)\rangle \tag{1.19}$$

by differentiating this equation we get,

$$\frac{d|\phi(t)\rangle}{dt} = \frac{\iota}{\hbar} e^{(\frac{\iota \hat{H}_0 t}{\hbar})} |\psi(t)\rangle + e^{(\frac{\iota \hat{H}_0 t}{\hbar})} \frac{|\psi(t)\rangle}{dt} \tag{1.20}$$

then on multiplying $\iota\hbar$ both side and by further solving, we finally get [19]

$$\iota\hbar \frac{d|\phi(t)\rangle}{dt} = \hat{H'}_1 |\phi(t)\rangle \tag{1.21}$$

1.7.2 Rotating frame

For a single-spin external Hamiltonian can be written as

$$\hat{H}_{lab} = \hat{H}_{zeeman} + \hat{H}_{rf} \tag{1.22}$$

$$\hat{H}_{lab} = -\hbar\omega_0 \hat{I}_z - \hbar\omega_1 [\hat{I}_x cos(\omega_{rf} t) + \hat{I}_y sin(\omega_{rf} t)] \tag{1.23}$$

By combining above equation by using rotation-sandwich relations as

$$\hat{H}_{lab} = -\hbar [e^{-\iota\omega_{rf} t} (\omega_0 \hat{I}_z + \omega_1 \hat{I}_x) e^{\iota\omega_{rf} t}] \tag{1.24}$$

Transforming the new state by following rule as

$$|\psi'(t)\rangle = e^{\iota\omega_{rot}t\hat{I}_z}|\psi(t)\rangle \tag{1.25}$$

whose dynamics is given by

$$\iota\hbar\frac{d|\psi'(t)\rangle}{dt} = \hat{H}'|\psi'(t)\rangle \tag{1.26}$$

where effective Hamiltonian is given as $\hat{H}'$

$$\hat{H}' = \hbar(\omega_0 - \omega_{rot})\hat{I}_z - \hbar\omega_1\hat{I}_x \tag{1.27}$$

therefore, $\omega_0 = \omega_{rot}$ is called on resonance condition and therefore, magnetisation in rotating frame will be in x-direction [19].

1.8 Relaxation

Spin-1/2 particle having magnetic moment $\vec{\mu}$ in a static magnetic field has two energy states separated by $\Delta E{=}2\vec{\mu}B$. If the spin-1/2 nuclei are placed in the static magnetic field (along the z-axis) for a long time, it reaches in the state of thermal equilibrium. At thermal equilibrium, the population of spins in each state is given by Boltzmann distribution. There will be more spins in the lower energy states than in the upper states, and the population difference gives rise to a magnetization $\vec{M}_z$.

Radio-frequency (R.f.) pulses disturb the equilibrium of the spin system [11, 19]. The population after a pulse usually deviate from their thermal equilibrium values, for example, a $\pi/2$ pulse equalizes spin state population whereas π pulse inverts the population distribution.

Relaxation is the process by which equilibrium is regained, through the interaction of the spin system with the thermal molecular environment. The study of nuclear spin relaxation is vital for several reasons [11, 19].

- Many motional processes in a molecule may be studied by nuclear spin relaxation.
- Nuclear spins relaxation is sensitive to non-secular spin interactions. The study of relaxation can reveal these 'hidden' spin interactions, which have little effect on the ordinary NMR spectrum.

Relaxation process can be divided into two types: Longitudinal relaxation (T_1) and Transverse relaxation (T_2).

1.8.1 Longitudinal relaxation (T_1)

At equilibrium, the net magnetization is along +z. R.f pulse disturbs the magnetization. The rate at which z magnetization recovers to its equilibrium value is characterized by a time constant T_1 that is called longitudinal relaxation. Longitudinal relaxation T_1 also called the spin-lattice relaxation.

1.8.2 Measuring T_1

The are various methods to measure T_1 relaxation. Commonly used methods are inversion recovery method and saturation recovery method.

Inversion recovery method

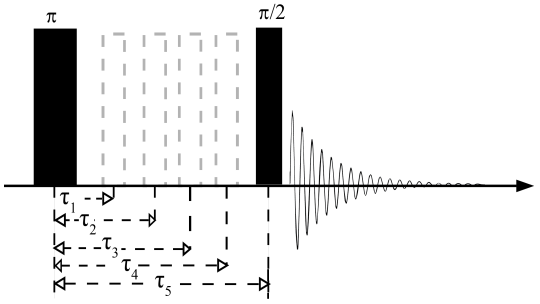

Figure 1.5: Pulse sequence schematic showing the inversion recovery experiment. The gray dotted lines are $\pi/2$ pulses that occur at different τ values [14].

In order to measure T_1, π pulse is applied that inverts the equilibrium magnetisation (+z magnetisation, M_{zo}) and creates -z magnetisation (-M_{zo}), which will decay back to +z (M_{zo}). Relaxation with time τ occurs according to following equation [20]:

$$M_z(\tau) = M_{zo}(1 - 2exp(-\tau/T_1)) \tag{1.28}$$

It can easily be verified from this equation that at $\tau = 0$ (immediately after the π pulse), $M_z(0)$= -$M_z(0)$, and as $\tau \to \infty$, $M_z(\infty) \to +M_z(0)$. But in order to detect the +z and -z magnetisation, the net magnetisation must be rotated into xy-plane [20].

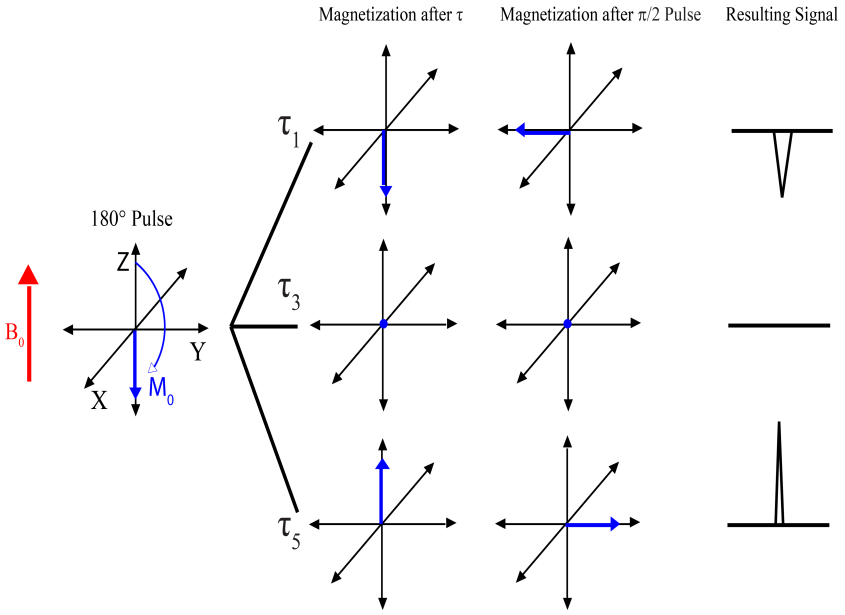

Figure 1.6: A graphic depicting the how the bulk magnetization changes with varying delays and pulses. The signal is first inverted and once the delay between the pulses is sufficient, the magnetization becomes positive [14].

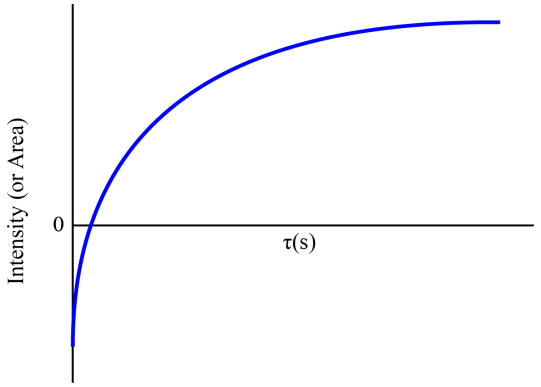

Figure 1.7: A plot of the intensity vs the delay times of the experiment [14].

1.8.3 Transverse relaxation (T_2)

$\pi/2$ rf pulse bring the +z magnetisation vector into xy plane. Then net magnetisation starts decaying in xy plane. The rate at which xy-magnetisation decays to zero is characterised by a time constant T_2 that is called transverse relaxation. Transverse relaxation also called spin-spin relaxation.

1.8.4 Measuring T_2

Carr-Purcell-Meiboom-Gill (CPMG) sequence

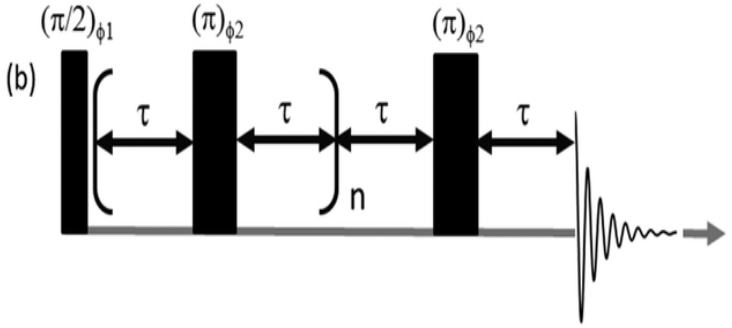

Figure 1.8: CPMG sequence for measuring T_2 [10].

In order to measure T_2 using CPMG, equilibrium magnetisation has to be rotated into xy-plane via $\pi/2_x$ pulse. After this record the spectrum at different values for τ. Here T_2 relaxation occurs according to the following equation [20]:

$$M_{xy}(\tau) = M_{zo}exp(-\tau/T_2) \tag{1.29}$$

It is simple to verify from this equation that at $\tau = 0$ (immediately after the $\pi/2$ pulse), $M_{xy}(0) = M_{zo}$, and as $\tau \to \infty$, $M_{xy}(\infty) \to 0$.

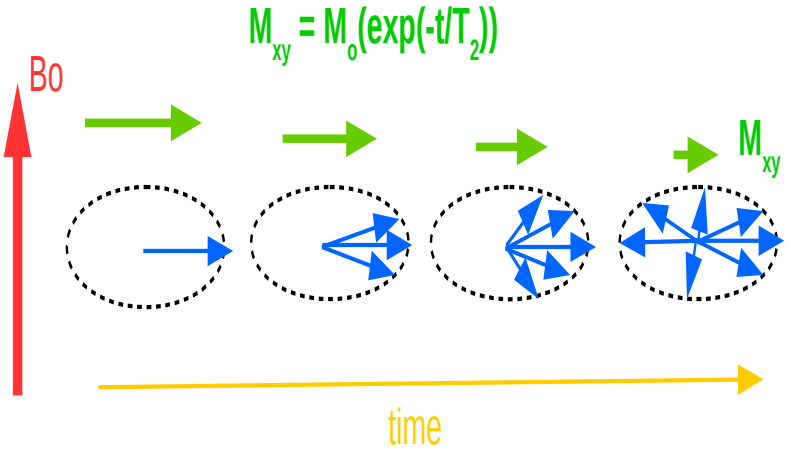

Figure 1.9: A graphic depicting how the bulk magnetization changes with varying delays.

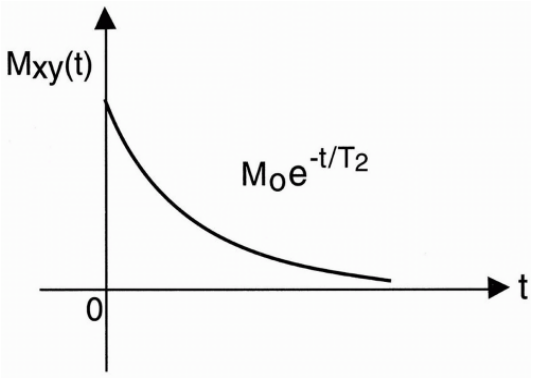

Figure 1.10: A plot of the intensity vs the delay times of the experiment [10].

Chapter 2

Diffusion and Pulsed field gradient NMR

2.1 Introduction

Translation motion (e.g., diffusion, flow) in solution is very significant and plays a crucial role in science. Diffusion studies can be applicable for vast scientific studies ranging from diseases to separation science and nano-technology. Further, the translation motion of a species not only reflects intrinsic properties of the species itself (e.g., hydrodynamics) but also provide information about the surrounding environment (e.g., inter-molecular dynamics or motional restriction). The study and understanding of translational motions of molecules and the molecular system have a great scientific value.

There are various difficulties that one encounter during measurement of translational motion at the molecular level. Specially, thermodynamic gradient (which leads to mutual diffusion and consequently irreversible thermodynamics) and the measurement of diffusion of species quite high concentration in the measurement process can have adverse effects on the outcome. Fortunately, nuclear magnetic resonance (NMR) provides a convenience way for performing non-invasive measurements of translation motion [21, 22, 15].

2.2 Diffusion

Diffusion can be defined as the random translational motion of particles that happens due to their internal energy. This random translational motion, i.e., Diffusion leads to

a collision between particles in a system and finally results in chemical reactions. It is one of the principal factor, other than activation energy and orientation, responsible for almost all chemical reactions since the reacting species must collide before they can react [3]. Diffusion can be more deeply understood by Fick's diffusion laws. There are two laws given by Adolf E. Fick; one is Fick's 1st law, and other is Fick's second law.

2.3 Fick's laws of diffusion

2.3.1 Fick's 1st law

Fick's 1st law of diffusion describes how particles under random thermal motion tend to spread from a higher concentration region to a lower concentration region [26]. This could be easily understood by an example when one opens a perfume bottle in the corner of a closed room. If he waits long enough, the perfume odor will spread throughout the room because the perfume molecules have diffused from one side of the room to the other, from a high concentration region to a low concentration region [23]. Mathematically, Fick's 1st diffusion law states that the diffusion flux is proportional to the concentration gradient, as:

$$\vec{J} = -D\nabla C(\vec{r}, t) \tag{2.1}$$

in case of one dimension,

$$J_x = -D\frac{\partial C(x,t)}{\partial x} \tag{2.2}$$

where

- $\vec{r}$ is the position vector.
- D is a constant known as diffusion coefficient. It is measured in the units of cm^2s^{-1} or m^2s^{-1}.
- C($\vec{r}$,t) is the concentration over space and time.
- $\vec{J}$ is the diffusion flux per unit area per unit time.
- t is the time in unit of second.

2.3.2 Fick's 2nd law

Fick's 2nd law states that change in the concentration of particles over time is equal to the change in local diffusion flux. In simple words, this law predicts how diffusion causes the concentration to change with respect to time. Mathematically, it can be expressed as:

$$\frac{\partial C(\vec{r},t)}{\partial t} = D\nabla^2 C(\vec{r},t) \tag{2.3}$$

in case of one dimension,

$$\frac{\partial^2 C(x,t)}{\partial t} = D\frac{\partial C(x,t)}{\partial x^2} \tag{2.4}$$

2.4 Stokes law

Stokes law states that the viscous force on a small sphere moving through a viscous fluid is directly proportional to the velocity of the sphere, the radius of the sphere, and the viscosity of the fluid [12]. Mathematically, this law can be written as:

$$F = 6\pi\eta r v \tag{2.5}$$

where

- r is the radius of the spherical object [m].
- v is the flow velocity relative to the object [m/sec].
- η is the dynamic viscosity of the medium [Pa-sec].
- F is the frictional force also known as Stokes' drag acting on the interface between the fluid and the particle.

2.5 Stokes-Einstein equation

The Stokes-Einstein equation is the equation derived by Einstein for the diffusion coefficient of a "Stokes" particle undergoing Brownian Motion in a stationary fluid at a uniform temperature.

$$D = \frac{k_B T}{6\pi\eta r} \tag{2.6}$$

where

- r is the radius of the spherical object [m].
- T is the temperature in [K].
- η is the dynamic viscosity of the medium [Pa-sec].
- k_B is Boltzmann constant [1.34*10^{-23} m^2kg s^{-2} K^{-1}].
- D is diffusion coefficient [m^2/sec].

2.6 Pulsed field gradient (PFG) NMR

- PFG-NMR provides a convenient and noninvasive means for measuring translational motion.
- Below is the PFG spin echo pulse sequence that is used to measure diffusion by observing the attenuation in NMR signal and its effect when there is no molecular molecular movement, diffusion, and unidirectional translation [18, 25].

,

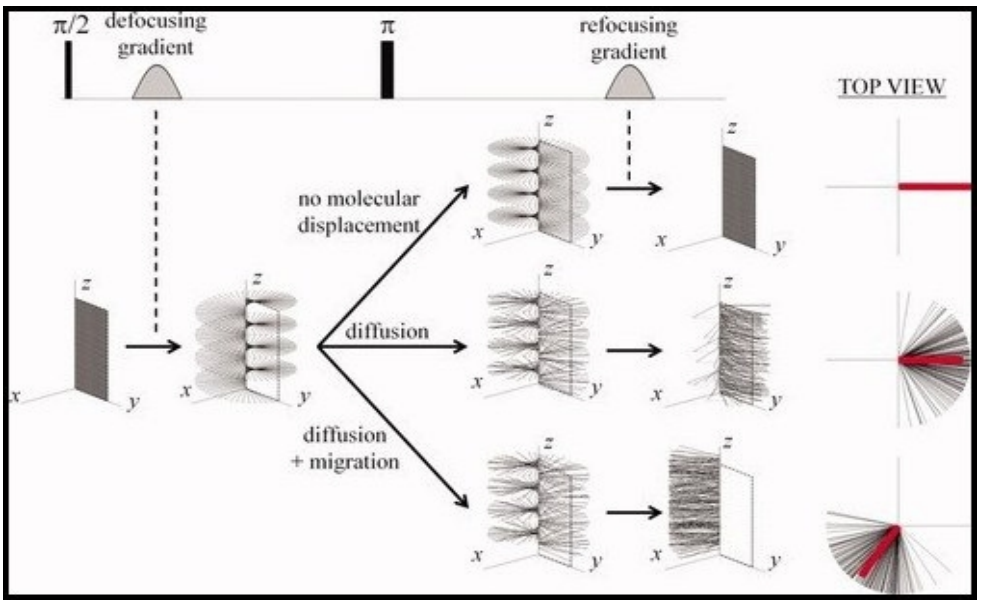

Figure 2.1: PFG spin echo pulse sequence [25].

Stejskal Tanner (ST) equation

The ST equation describes the signal attenuation in PFGSE experiment due to loss of coherence during diffusion. And it is given by [8]

$$\mathbf{I/I_o = exp[-(\gamma\delta g)^2 D(\Delta - (\delta/3)]} \tag{2.7}$$

where

- I is the intensity of the signal.
- γ is the gyromagnetic ratio.
- δ is duration of gradient pulse [sec].
- g is the gradient strength [(Tesla/meter)^2].
- D is the diffusion coefficient [m^2/sec].

Chapter 3

Ionic Liquids

3.1 What are Ionic liquids?

Ionic liquids (ILs) are the salt, having a low melting point (generally below 373 k) that's why found in a liquid state at ambient temperatures. ILs have received great interest because of their unusual properties as liquids. ILs exist as liquids at ambient temperatures because of their chemical structure. The anion and cation are chosen precisely to destabilize the solid-phase crystal. Thus, while there are no set rules to making an IL, in general, this can be achieved within a relatively large window of ion structures by balancing ion-ion interactions and symmetry as shown in Figure (3.1). For instance, the cation alkyl chain must be long enough to reduce Coulombic forces and disrupt lattice packing, but not be too long (number of carbon atom < 12) as this will increase salt melting point despite the enhanced asymmetry; cohesive interactions increase with length of nonpolar groups as per linear alkanes. ILs are largely made of ions and short lived ions, while ordinary liquids such as water and gasoline are predominantly made of neutral molecules.

3.2 ILs as Electrolytes

If we look into the past, we would found that organic solvents were used as an electrolyte in various electrical energy storage devices such as batteries. There are various limitations of organic solvents that limits there further use such as high volatility, flammable, generation of poisonous gas and low chemical and thermal stability. So, currently the people has started using ILs as electrolyte in electrical energy storage devices, the best examples are Lithium-ion battery, super capacitors and many

Table 3.1: **Basic characteristics of Ionic Liquids.**

Low melting point	(i) Treated as a liquid at ambient temperature (ii) Wide usable temperature range
Non-volatility	(i) Thermal stability (ii) Chemical stability (iii) Nonflammable
Compose by ions	(i) High ion density
Organic ions	(i) Various kinds of salts (ii) Designable (iii) Unlimited combinations

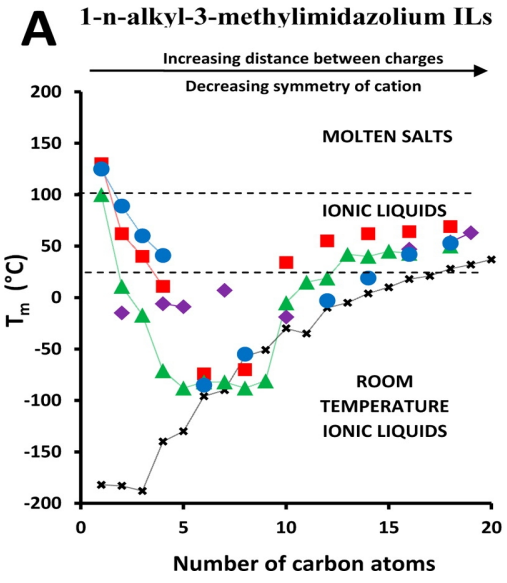

Figure 3.1: Melting point (T_m) as a function of cation alkyl chain length (n) for salts systems with 1-n-alkyl-3-methylimidazolium cations. The trend in T_m is consistent across all salts: low n values $T_m > 100$ °C; intermediate n values 50 °C $< T_m <$ 100 °C then $T_m < 25$ °C; and large n values 50 °C $< T_m <$ 100 °C. Dashed lines indicate the boundaries between molten salts ($T_m > 100$ °C) ILs ($T_m \leq 100$ °C) and RTILs ($T_m \leq 25$ °C) [5].

more. This is because ILs have several advantages over organic solvents. They have low volatility, nonflammable, recyclability and chemically and thermally stable. ILs unique properties have made them promising green solvents to replace traditional solvents such as DMAc/LiCl and DMSO/TBAF [13].

3.3 Dissociation constant of ILs using Diffusion Coefficient

ILs normally contains three components in the liquid states: cation, anion and ion-pair (neutral molecule) [13]. The thermal and kinetic behavior of ILs are strongly dependent on their ions concentration.

The dissociation constant (K_d) calculated from the diffusion coefficient of ions measured by NMR is from not only ionized cations and anions but also unionized ion-pairs. The ionization process of ILs can be expressed as

$$\begin{array}{ccccc} Ion-pair & \leftrightarrows & cation & + & anion \\ (1-x) & & x & & x \\ D_{ip} & & D_c & & D_a \end{array}$$

where x is the ion concentration fraction, and D_{ip}, D_c, D_a are the self-diffusion coefficient of ion-pair, cation, and anions respectively. The observed self-diffusion coefficient of cation, $D_{c,obs}$ from NMR is actually the average of ionized cation and ion-pair diffusion coefficient. Similarly, the observed self-diffusion coefficient of anion $D_{a,obs}$ is the average of the ionized anion and ion-pair diffusion coefficient.

$$D_{c,obs} = xD_c + (1-x)D_{ip} \tag{3.1}$$

$$D_{a,obs} = xD_a + (1-x)D_{ip} \tag{3.2}$$

The equations (3.1) and (3.2) can be rewritten as

$$x = (D_{c,obs} - D_{a,obs})/(D_c - D_a) \tag{3.3}$$

From equation (3.3) if $D_{c,obs}$, $D_{a,obs}$, D_c and D_a are Known, x can be obtained. In addition the equilibrium constants of ionization process can be calculated from x as

$$K_d = x^2/(1-x) \tag{3.4}$$

$D_{c,obs}$ and $D_{a,obs}$ can be obtained directly from the Pulsed Field Gradient (PFG) NMR measurement.

Under the assumption that ions in ionic liquids are completely dissociated at high temperature, it is possible to obtain D_c and D_a by fitting the linear parts of the Arrhenius plots of $D_{c,obs}$ and $D_{a,obs}$ at high temperature (as shown in figure (3.3)) [13]. The Arrhenius relation that shows the temperature dependency of diffusion can be expressed as

$$D_c = D_{oc} e^{-E_c/RT} \tag{3.5}$$

and

$$D_a = D_{oa} e^{-E_a/RT} \tag{3.6}$$

where E_c, E_a are the activation energies for self-diffusion of cations and anions respectively, D_{oc} and D_{oa} are pre-exponential factor of cations and anions respectively.

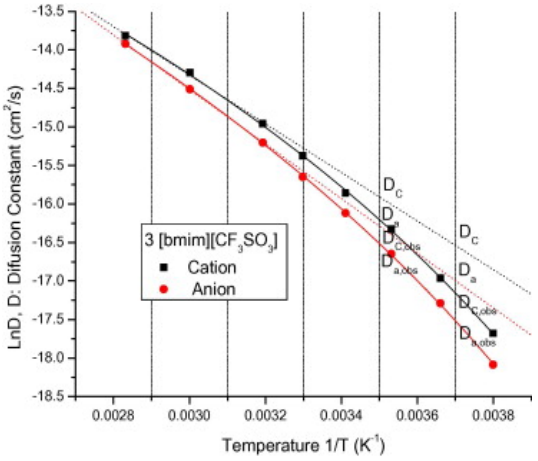

Figure 3.2: The plot of lnD vs. 1/T for [bmim][CF_3SO_3] and fitting lines [13].

Chapter 4

Experimental methods, result and discussion

4.1 Ionic Liquids

These four ILs (shown in figure 4.1) were purchased from Sigma-Aldrich company. We choose these four ILs because of their importance in current research and their applications. Like "Lithium bis(trifluoromethane) sulfonnyl imide" is used as an electrolyte in Lithium ion batteries and "imidazolium salts" are very much popular in scientific research based on ILs and so on.

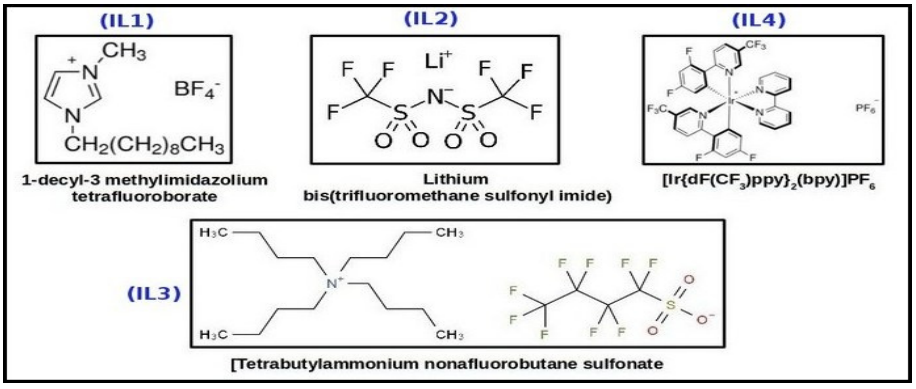

Figure 4.1: These are four pure ionic liquids that we have for our study.

4.1.1 Properties and Notations used for ILs

Ionic liquids are used as electrolytes in various electrical energy storage devices such as lithium-ion batteries. There are various outstanding properties of ILs like a less

Table 4.1: **Properties of ILs and Notations used for them. where MW is Molecular weight.**

Name of ionic liquid	Notation used	MW (g/mole)	Properties
1-Decyl, 3-methylimiddazolium tetrafluoroborate	IL1	310.18	Hygroscopic, Soluble in alcohol.
Lithium bis(trifluoromethan) sulfonyl imide	IL2	287.09	Hygroscopic, Density=1.33 g/cm3, Soluble in water
Tetrabutyl ammonium nona-fluorobutane sulfonate	IL3	541.56	Hygroscopic, Solube in water and alcohol
[Ir{dF(CF3)ppy}2(bpy)]PF6	IL4	1009.7	Hygroscopic

volatile, nonflammable, highly chemically and thermally stable. However, the problem with pure ionic liquid is that their ionic conductivity is a little low. If their ionic conductivity can be increased, then the electrical energy storage capacity of these devices can be increased. In order to see an increase in ionic conductivity, we prepare a mixture of various ionic liquids. Moreover, trying to calculate the dissociation constant via diffusion coefficient (that we measure using PFG-NMR). Following are the equations that we use: The ionization process of ILs can be expressed as

$$\begin{array}{ccccc} Ion-pair & \leftrightarrows & cation & + & anion \\ (1-x) & & x & & x \\ D_{ip} & & D_c & & D_a \end{array}$$

$$D_{c,obs} = xD_c + (1-x)D_{ip} \tag{4.1}$$

$$D_{a,obs} = xD_a + (1-x)D_{ip} \tag{4.2}$$

$$x = (D_{c,obs} - D_{a,obs})/(D_c - D_a) \tag{4.3}$$

$$K_d = x^2/(1-x) \tag{4.4}$$

- Notations like IL12, IL23, IL34 and so on were also used, where IL12 represent the mixture of pure IL1 and Pure IL2 and similarly for others.

4.2 Sample preparation

- Generally ILs are hygroscopic, they easily capture moisture from the surrounding environment. In order to remove water content from ILs, we perform vacuum

dry at 0.049 mbar pressure and 60 °C temperature.

- Then, 20 mM concentration solution of each pure ILs was prepared in methanol-d_4 solvent.
- to prepare the solution for IL12 (a mixture of pure IL1 and IL2), an equal volume of 20 mM solution of each IL1 and IL2 were added. Moreover, did the same for other ILs like IL23, IL34, and so on.
- In order to record NMR spectra, 200 ul solution of IL was taken in a 3 mm NMR tube. Further, this 3mm NMR tube was inserted into 5 mm NMR tube containing D_2O.

4.3 NMR spectra for various ILs

NMR spectra is very much essential to now qualitatively change around the environment of nuclei. Firstly, we recorded the NMR spectra of all pure ILs and their mixture as shown in figure (4.3.1) and figure (4.3.1).

4.3.1 ^1H NMR spectra

For pure ILs

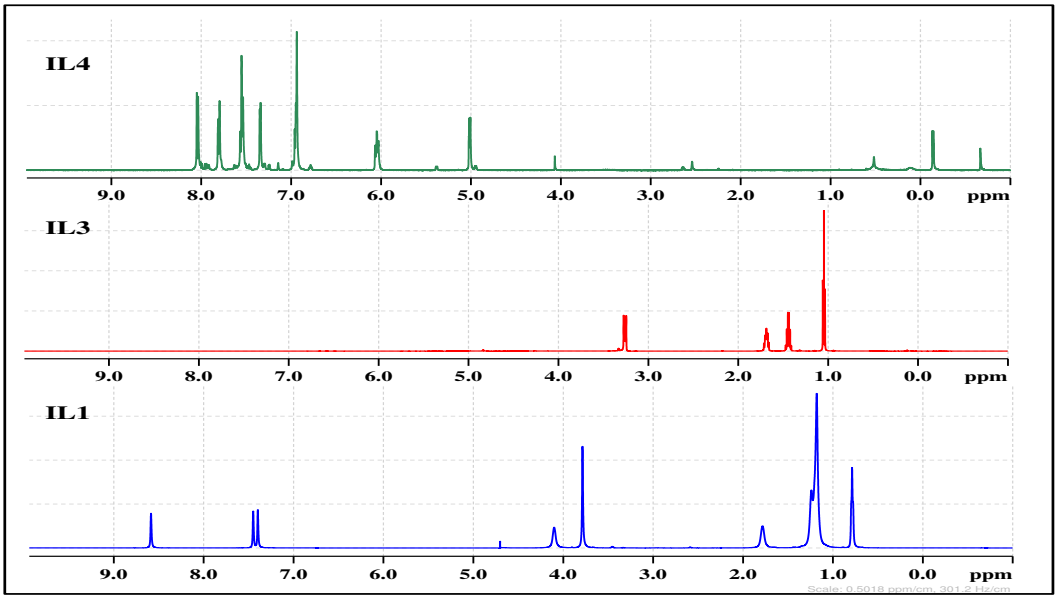

Figure 4.2: ^1H-NMR spectra of pure ionic liquids.

For binary mixture of ILs

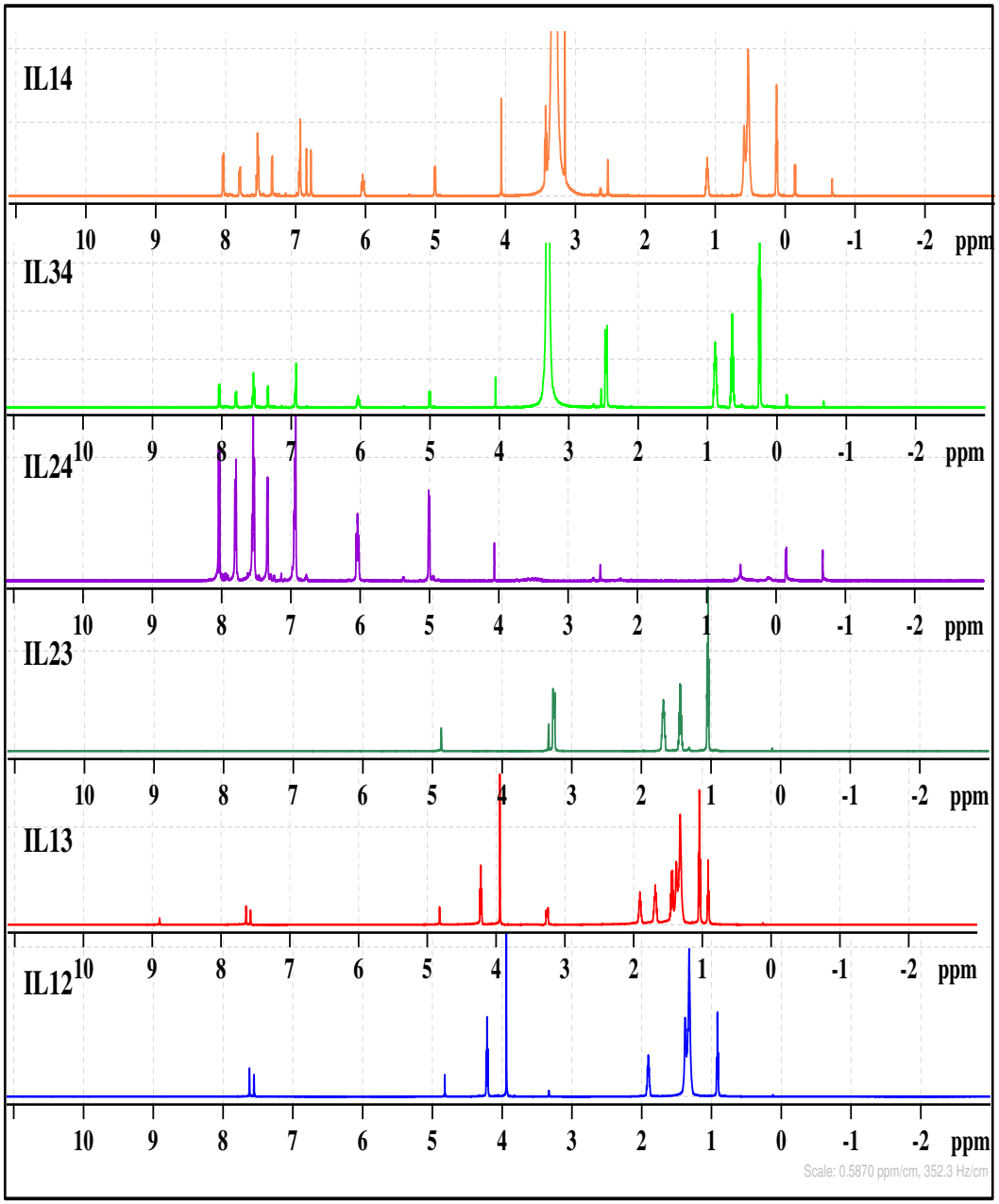

Figure 4.3: ^1H-NMR spectra of binary mixture of ionic liquids. Where IL13 represents the mixture of pure IL1 and IL3 and similarly for others.

On comparing the spectra of pure ILs with the spectra of mixtures, we observed a shift in the peaks that suggest the change in the environment around nuclei.

4.3.2 ^{19}F NMR spectra

For binary mixture of ILs

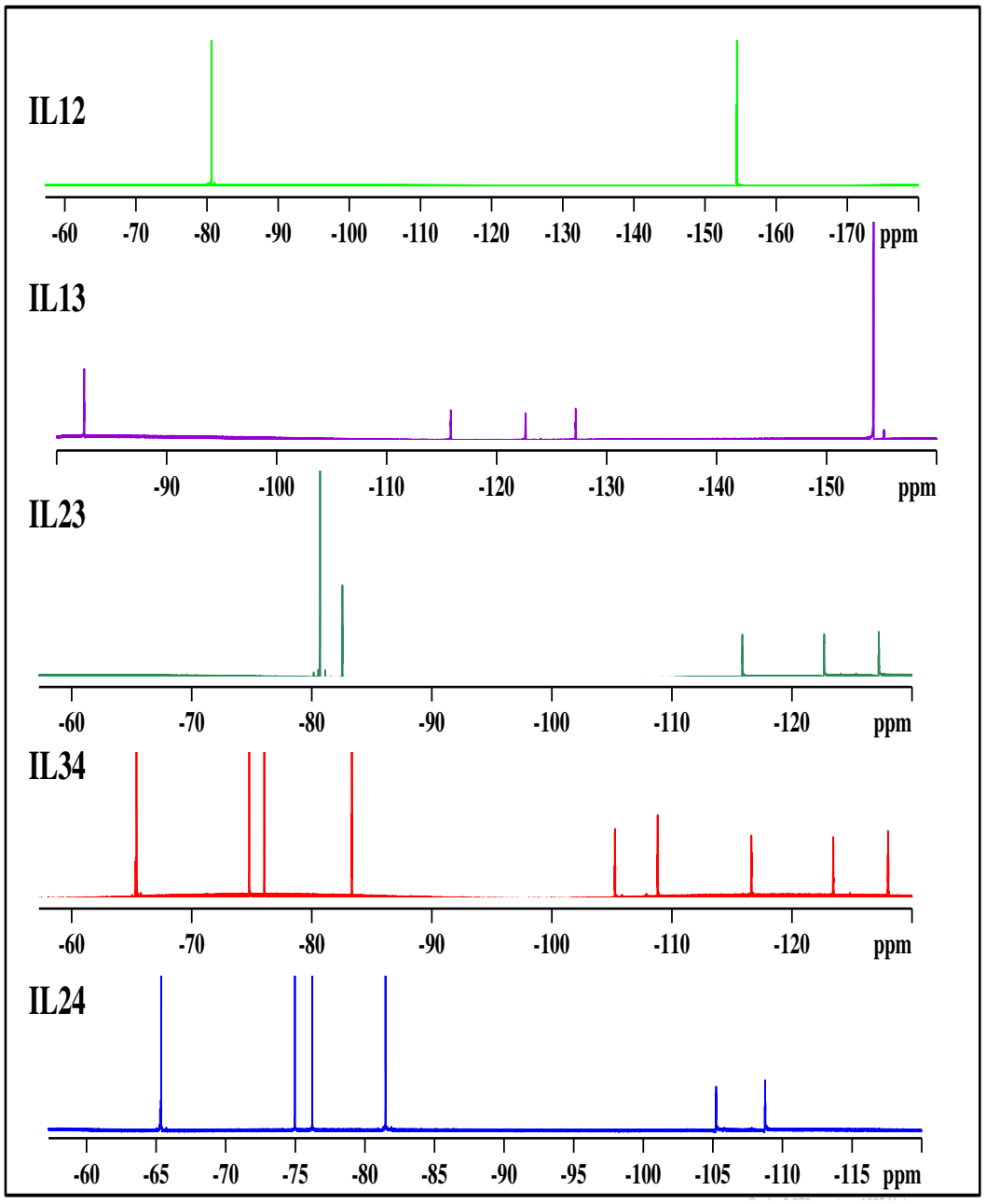

Figure 4.4: ^{19}F-NMR spectra for binary mixture of ILs.

For pure ILs

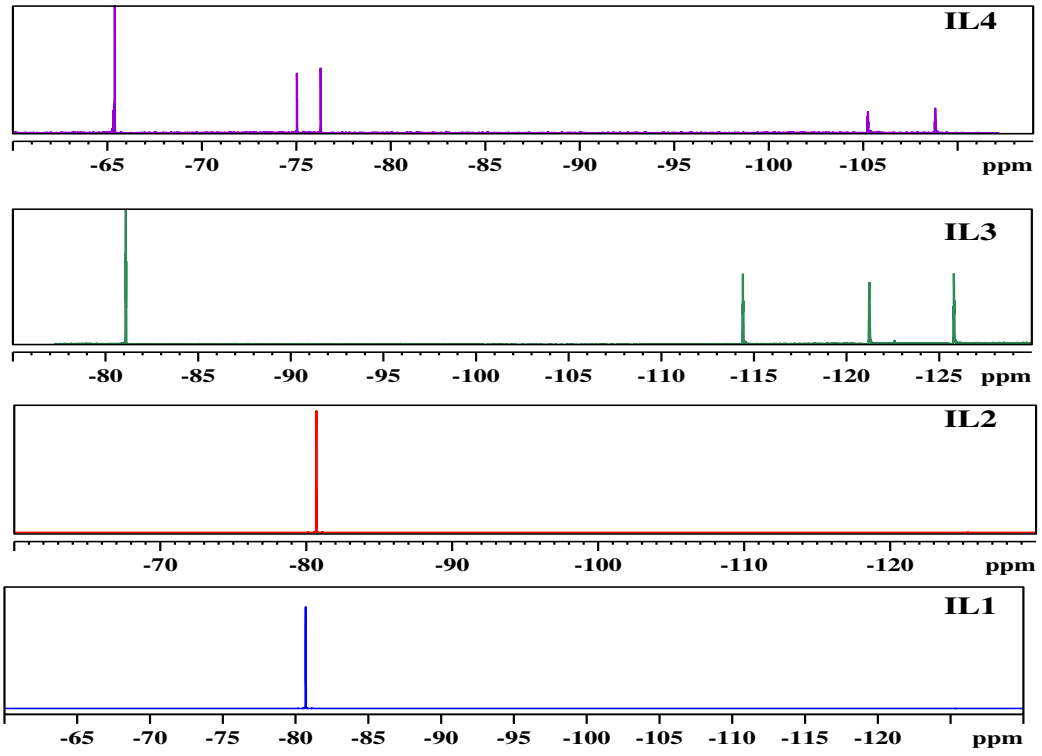

Figure 4.5: ^{19}F-NMR spectra of pure ILs.

4.4 T_1 and T_2 measurement

Longitudinal relaxation (T_1)

S. No.	Ionic liquids	Peak Value (in ppm)	T1 (in sec.)
1.	IL1	p1 = 8.60	0.850 ± 0.009
2.	IL2	p1 = 1.91	1.807 ± 0.018
3.	IL3	p1 = 1.04	1.621 ± 0.016

Table 4.2: Longitudinal relaxation (T_1) values of pure ILs calculated using inversion recovery method.

T_1 and T_2 were measured using inversion recovery method and CPMG sequence method respectively. T_1 and T_2 values tells us that how fast or slow spin relaxes.

S. No.	Ionic liquids	Peak value (in ppm)	T1 (in sec.)
4.	IL12	p1 = 1.910	1.086 ± 0.011
5.	IL13	p1 = 1.042	1.745 ± 0.017
		p2 = 4.222	1.486 ± 0.015
6.	IL23	p1 = 1.042	1.615 ± 0.016
		p2 = 4.840	6.228 ± 0.061

Table 4.3: Longitudinal relaxation (T_1) values of mixtures of ILs calculated using inversion recovery method.

The T_1 values are given in Table (4.4) (for pure ILs) and Table (4.4) (for mixtures) respectively. We observed that T_1 values for mixtures are slight higher that T_1 values for pure ILs. This also suggest change in the dynamics of the system.

4.5 Homo-nuclear Correlation Spectroscopy (COSY) spectra

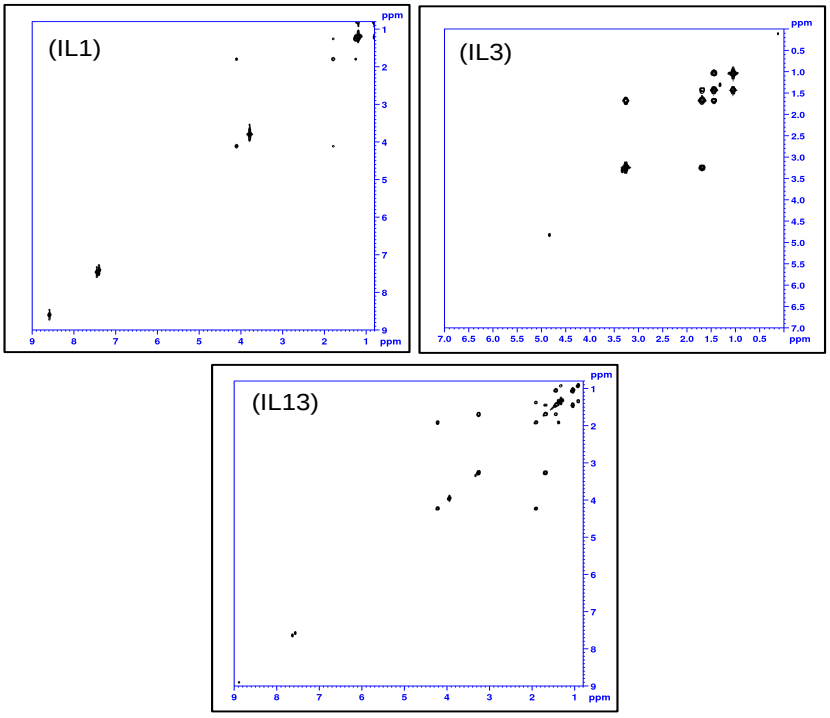

Figure 4.6: 2D homo-nuclear COSY spectra of IL1, IL3 and IL13.

4.6 Diffusion Experiments

4.6.1 For ^1H nuclei

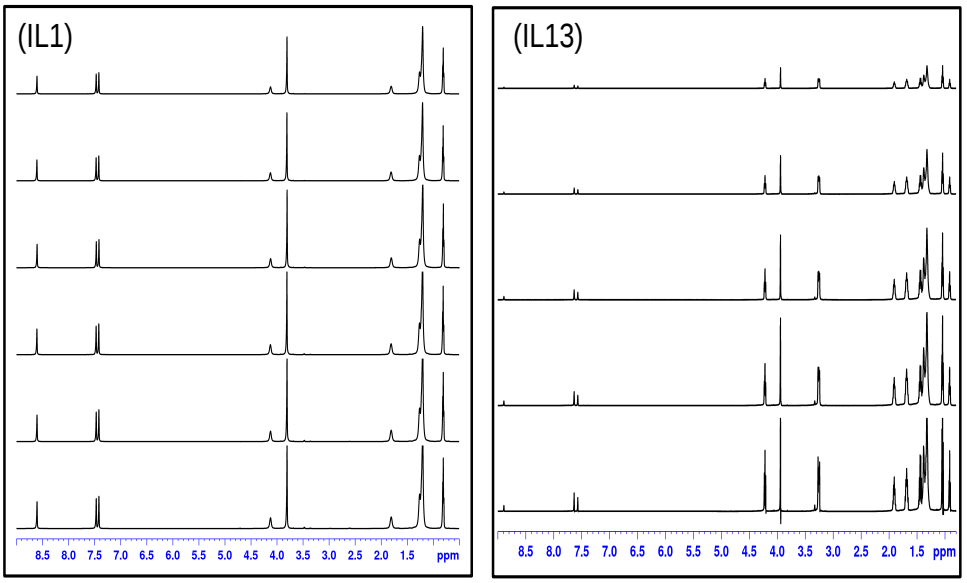

Figure 4.7: 1D-Diffusion spectra of IL1 and IL13 (with decreasing gradient strength).

PFG-NMR spectra for all ILs

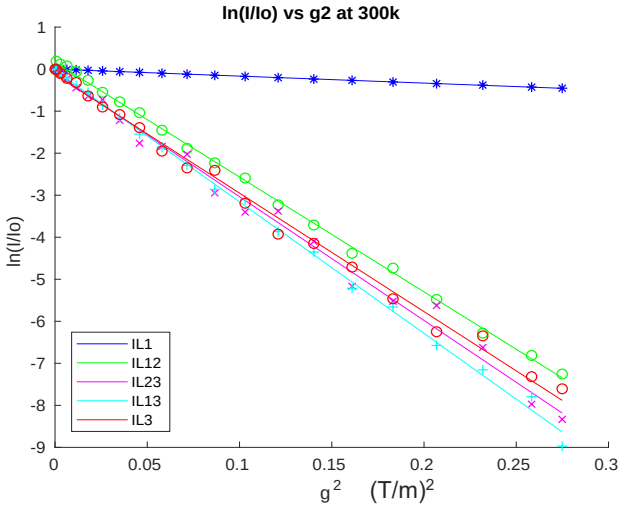

Figure 4.8: Comparison of diffusion coefficient for various ILs at 300 k. Here, slope represent the diffusion constant, more the value of slope higher the diffusion coefficient.

S. No.	Ionic liquids	Peak value (in ppm)	Diffusion coefficient (in mˆ2/sec.)
1.	IL1	p1 = 0.806	1.147*10ˆ(-10)
		p2 = 1.800	1.097*10ˆ(-10)
		p3 = 8.600	1.074*10ˆ(-10)
2.	IL2	p1 = 1.305	4.100*10ˆ(-8)
		p2 = 1.909	4.623*10ˆ(-8)
		p3 = 3.331	7.582*10ˆ(-8)
3.	IL3	p1 = 1.684	3.915*10ˆ(-8)
		p2 = 3.250	3.914*10ˆ(-8)
4.	IL12	p1 = 1.904	3.767*10ˆ(-8)
		p2 = 0.908	3.793*10ˆ(-8)
		p3 = 3.341	16.37*10ˆ(-8)
5.	IL13	p1 = 8.902	4.421*10ˆ(-8)
		p2 = 0.909	4.346*10ˆ(-8)
		p3 = 1.684	4.010*10ˆ(-8)
		p4 = 1.912	4.389*10ˆ(-8)
		p5 = 3.250	4.038*10ˆ(-8)
6.	IL23	p1 = 1.684	4.042*10ˆ(-8)
		p2 = 3.250	4.058*10ˆ(-8)

Table 4.4: Diffusion coefficients values for various ILs calculated using PFG-NMR.

Diffusion coefficients for various ILs were calculated using Pulsed Field Gradient (PFG) sequence. Above figure (4.7) shows the output of the PFG experiment for IL1 and IL13. while performing PFG experiment, gradient strength were changed to record the intensity plot. The graphs in the figure (4.7) are arranged in such a way that the the gradient strength increases as we move up in the figure (4.7). It is observed that as the gradient strength increases the intensity of the peak reduces (or the height of the peak reduces).

In figure (4.8), log(I/I$_o$) Vs. g^2 plots were plotted for IL1 (blue), IL12 (green), IL23 (magenta), IL13 (cyan) and IL3 (red) at 300 k temperature. Here, the slope of the graph represent the diffusion coefficient, so the plots in figure (4.8) helps us to compare the diffusion coefficient values. Further in the Table (4.4), diffusion coefficient values shown that were calculated using PFG-NMR.

4.6.2 For ^7Li nuclei

In order to calculate the dissociation constant (K$_d$), we need diffusion coefficient (D) value for each anion and cation. That's why we also have to calculate the D value for

some ILs, mainly containing Lithium (^7Li) nuclei (like IL2, IL12, IL23 and IL24).

PFG-NMR spectra for all ILs

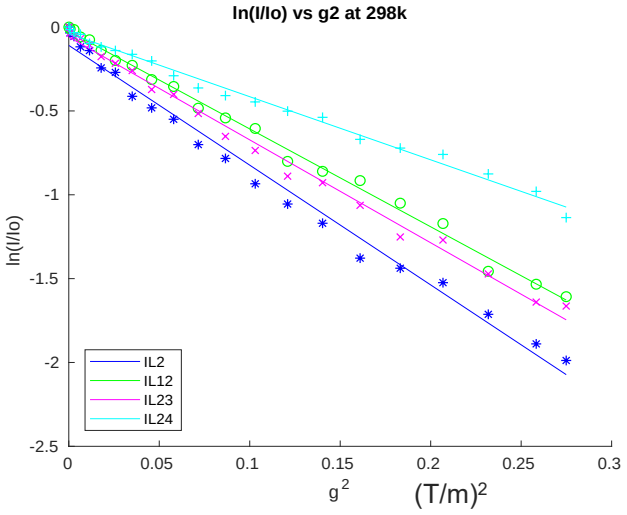

Figure 4.9: Comparison of diffusion coefficient for various ILs at 298 k.

Temperature effect on diffusion

For IL2

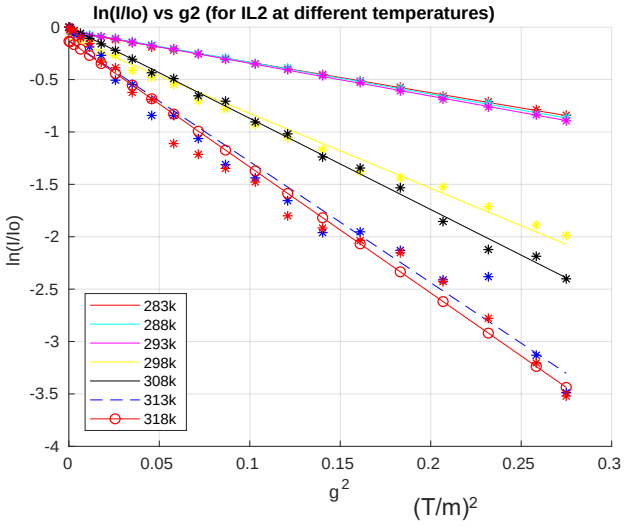

Figure 4.10: Diffusion coefficient For IL2 at different temperature.

For IL12

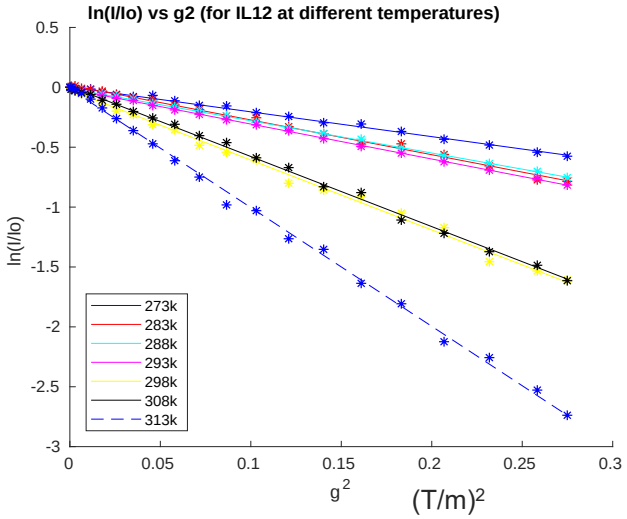

Figure 4.11: Diffusion coefficient For IL12 at different temperature.

In figure (4.10), (4.11), (4.12) and (4.13), log(I/I_o) Vs. g^2 plots were plotted for IL2, IL12, IL23 and IL24 at different temperatures.

For IL23

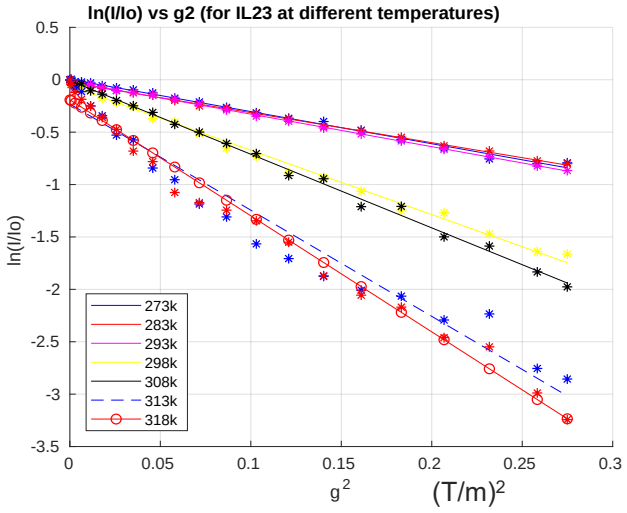

Figure 4.12: Diffusion coefficient For IL23 at different temperature.

For IL24

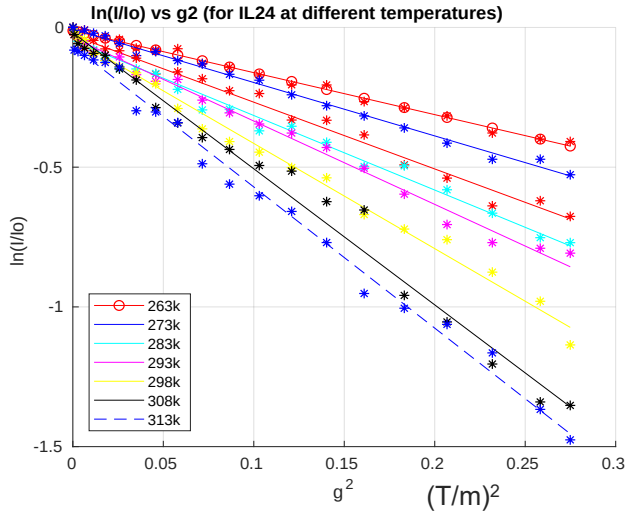

Figure 4.13: Diffusion coefficient For IL24 at different temperature.

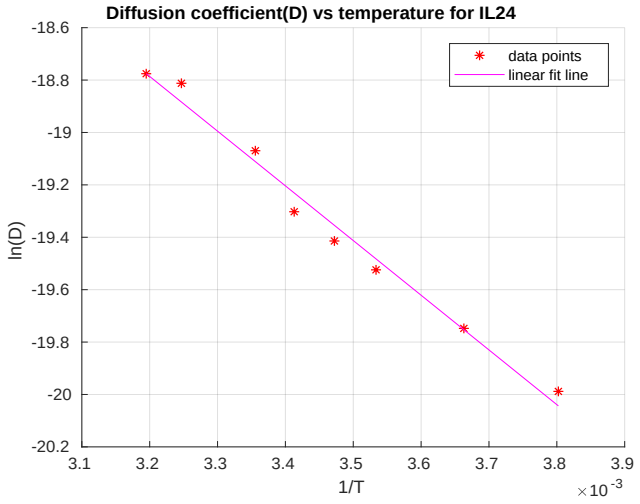

Figure 4.14: ln(D) Vs. 1/T plot. D and T are in the units of m^2/sec and kelvin(K) respectively.

This suggests that the diffusion coefficient increases with an increase in the temperature and follows the Arrhenius relation:

$$D_a = D_{oa} e^{-E_a/RT} \tag{4.5}$$

4.6.3 For ^{19}F nuclei

PFG-NMR spectra for ILs

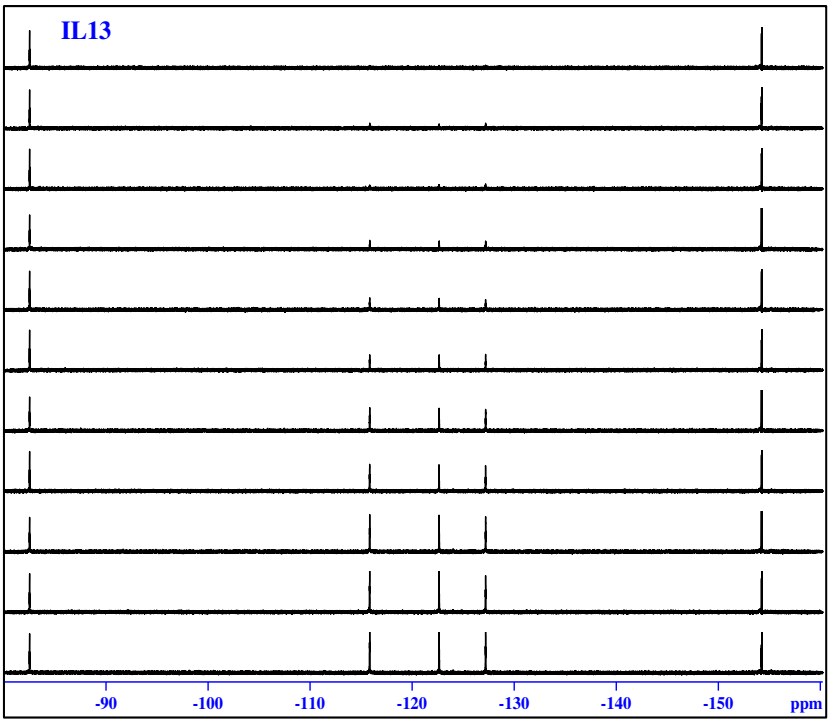

Figure 4.15: 1D-Diffusion spectra (^{19}F) of IL13(with decreasing gradient strength).

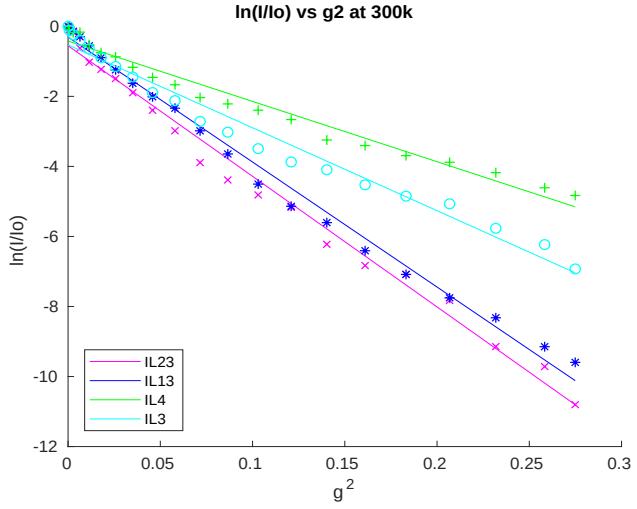

Figure 4.16: Comparison of diffusion coefficient for various ILs at 300 k.

4.7 Conclusion and Future Direction

NMR spectroscopy is a versatile technique to identify the structure of various biological and chemical species. The comparison of ^1H NMR spectra of Pure ILs as shown in figure (4.3.1) with the binary mixture of ILs as shown in figure (4.3.1) displays the shifts in the peaks that suggest us that the change in the environment around nuclei has occurred due to mixing. We provided the T_1 values for pure ILs as well as for mixtures. Slightly higher T_1 values for mixtures of ILs shows us that the dynamics of the molecules has increased.

Also, the plots of $\log(I/I_o)$ Vs. g^2 for various ILs at 298k were provided that helps us to compare the diffusion coefficient of ILs. As in figure (4.16) we see that pure ILs has the highest slope so as the diffusion coefficient, after mixing IL2 with other ILs (like IL1, IL3, and IL4) we observe the decrease in the slope so as the diffusion coefficient.

Also, diffusion coefficient values for ILs containing ^7Li nuclei (IL2, IL12, IL23, and IL24) were calculated at different temperatures ranging from 263K to 318K to observe the effect of temperature on diffusion coefficient. With the increase in the temperature, the increase in diffusion coefficient was observed. Figure (4.14) displays that the diffusion follows the Arrhenius profile with temperature.

Finally, ionic liquids are gaining more importance because of there outstanding properties, wide application and easy to tune their physical properties by simple means like mixing (as we have exploited in this work).

Appendix A

Derivation of Stokes-Einstein Equation

The motion of a particle moving along x-axis under constant external force F_{ext} can be expressed as

$$\frac{dv_x}{dt} = \frac{F_{ext}}{m} \tag{A.1}$$

where v_x is the velocity along x, and m is the mass of particle. on solving further,

$$v_x(t) = v_{0,x} + \frac{F_{ext}}{m} \tag{A.2}$$

$$\Delta x = v_{0,x} + \frac{F_{ext(\Delta t)^2}}{m} \tag{A.3}$$

On taking average both side of the equation

$$< \Delta x >= \frac{F_{ext(\Delta t)^2}}{2m} \tag{A.4}$$

when friction force ($F_{vis} = 6\ \pi\eta v R$) become equal to external force (F_{ext}), the particle achieves a terminal velocity v_{ter}.

$$F_{vis} = F_{ext} \tag{A.5}$$

$$6\pi\eta v_{ter} R = F_{ext} \tag{A.6}$$

$$v_{ter} = \frac{F_{ext}}{6\pi\eta R} = \frac{F_{ext}}{f} \tag{A.7}$$

where

$$f = 6\pi\eta R \tag{A.8}$$

From equation (A.4), f can also be written as

$$f = \frac{2m}{\Delta t} \tag{A.9}$$

Also from diffusion law, diffusion coefficient can be written as

$$D = \frac{L^2}{2\Delta t} \tag{A.10}$$

Using equation (A.9) and (A.11),

$$fD = \frac{mL^2}{(\Delta t)^2} \tag{A.11}$$

$$fD = mv_{0,x}^2 \tag{A.12}$$

Also from equipartition theorem, we can write

$$< v_{0,x}^2 >= \frac{k_B T}{m} \tag{A.13}$$

on putting equation (A.13) into equation (A.12), we get

$$fD = k_B T \tag{A.14}$$

$$D = \frac{k_B T}{f} = \frac{k_B T}{6\pi\eta R} \tag{A.15}$$

This is the Stokes-Einstein equation.

Appendix B

Topspin Commands

Command	Functon
wrpa	To copy the experiment at desired location.
edc	To create a directory,
i	To copy the experiment.
rsh	To read the shim file.
rga	To set receiver gain.
zg	To start acquisition.
atma	To tune and match atomatically.
atmm	To tune and match manually.
getprosol	To set the default values in the experiment.
pulsecal	To calibrate pulse length automatically.
efp	Perform fourier processing.
apk	Automatic phase correction.
abs	Automatic base line correction.

Appendix C

Supplementary information

C.1 For ^1H nuclei

C.1.1 PFG-NMR spectra for all ILs

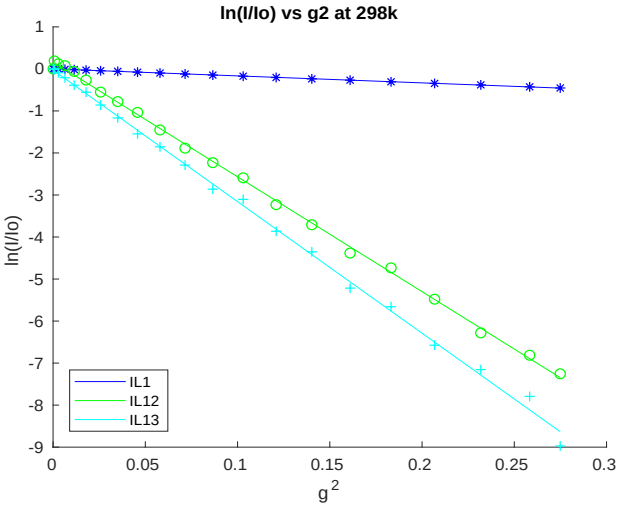

Figure C.1: Comparison of diffusion coefficient for various ILs at 298 k. Here, slope represent the diffusion constant, more the value of slope higher the diffusion coefficient.

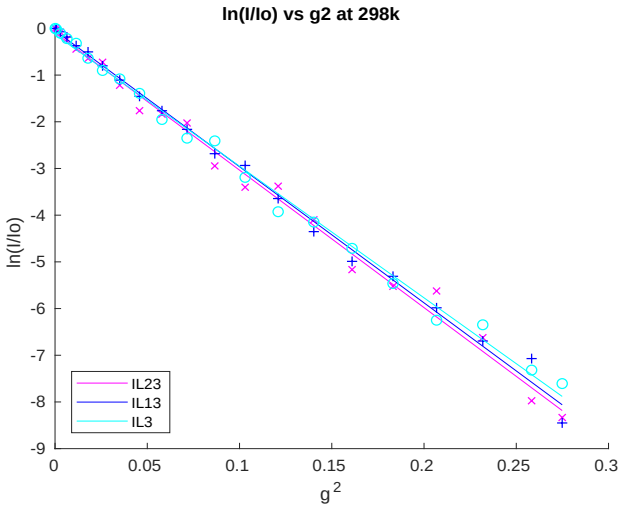

Figure C.2: Comparison of diffusion coefficient for various ILs at 298 k. Here, slope represent the diffusion constant, more the value of slope higher the diffusion coefficient.

Bibliography

[1] chem. latech. Nmr spectroscopy - theory. http://www.chem.latech.edu/7Eupali/chem281/281lab/NMR/NMRtheory.htm.

[2] K. Damodaran. Chapter four - recent nmr studies of ionic liquids. volume 88 of *Annual Reports on NMR Spectroscopy*, pages 215 – 244. Academic Press, 2016.

[3] P. Green. *Kinetics, Transport, and Structure in Hard and Soft Materials*. Taylor & Francis, 2005.

[4] H. Günther. *NMR spectroscopy: basic principles, concepts, and applications in chemistry*. Wiley, 1995.

[5] R. Hayes, G. G. Warr, and R. Atkin. Structure and nanostructure in ionic liquids. *Chemical Reviews*, 115(13):6357–6426, 2015. PMID: 26028184.

[6] R. P. Hicks. Nmr spectroscopy, second edition. basic principles, concepts and applications in chemistry edited by harald gunther (university of siegen). john wiley & sons, new york, ny. 1995. xx + 581 pp. 15 22.5 cm. isbn 0-471-95201-x. $39.95. *Journal of Natural Products*, 59(3):338–338, 1996.

[7] P. Hore, J. Jones, and S. Wimperis. *NMR: The Toolkit*. Ocp Series. Oxford University Press, 2000.

[8] M. I. Hrovat and C. G. Wade. Nmr pulsed-gradient diffusion measurements. i. spin-echo stability and gradient calibration. *Journal of Magnetic Resonance (1969)*, 44(1):62 – 75, 1981.

[9] J. Keeler. *Understanding NMR Spectroscopy*. Wiley, 2005.

[10] R. key. T2 relaxation. https://radiologykey.com/t1-t2-and-t2/.

[11] M. Levitt. *Spin Dynamics: Basics of Nuclear Magnetic Resonance*. Wiley, 2008.

[12] mae ulf. Stokes-drag-formula. http://www2.mae.ufl.edu/~uhk/STOKES-DRAG-FORMULA.pdf.

[13] Y. Mao and K. Damodaran. Ionization dynamics in ionic liquids probed via self-diffusion coefficient measurements. *Chemical Physics*, 440:87 – 93, 2014.

[14] Mindtouch. T1 relaxation. https://chem.libretexts.org/Bookshelves/Physical_and_Theoretical_Chemistry_Textbook_Maps/Supplemental_Modules_(Physical_and_Theoretical_Chemistry)/Spectroscopy/Magnetic_Resonance_Spectroscopies/Nuclear_Magnetic_Resonance/NMR/3A_Theory/Relaxation/Spin_Lattice_Relaxation.

[15] K. F. Morris and C. S. Johnson. Diffusion-ordered two-dimensional nuclear magnetic resonance spectroscopy. *Journal of the American Chemical Society*, 114(8):3139–3141, 1992.

[16] U. of Colorado. chemical shift. http://www.orgchemboulder.com/Spectroscopy/nmrtheory/chemshift.shtml.

[17] I. S. Oliveira, T. J. Bonagamba, R. S. Sarthour, J. C. Freitas, and E. R. deAzevedo. 2 - basic concepts on nuclear magnetic resonance. In I. S. Oliveira, T. J. Bonagamba, R. S. Sarthour, J. C. Freitas, and E. R. deAzevedo, editors, *NMR Quantum Information Processing*, pages 33 – 91. Elsevier Science B.V., Amsterdam, 2007.

[18] G. Pags, V. Gilard, R. Martino, and M. Malet-Martino. Pulsed-field gradient nuclear magnetic resonance measurements (pfg nmr) for diffusion ordered spectroscopy (dosy) mapping. *Analyst*, 142:3771–3796, 2017.

[19] S. Pascal. *NMR Primer: An HSQC-based Approach with Vector Animations*. IM Publications, 2008.

[20] S. Pascal. *NMR Primer: An HSQC-based Approach with Vector Animations*. IM Publications, 2008.

[21] W. Price and W. Price. *NMR Studies of Translational Motion: Principles and Applications*. Cambridge Molecular Science. Cambridge University Press, 2009.

[22] W. Price and W. Price. *NMR Studies of Translational Motion: Principles and Applications*. Cambridge Molecular Science. Cambridge University Press, 2009.

[23] science direct. Fick's law - an overview — sciencedirect topics. https://www.sciencedirect.com/topics/engineering/ficks-law.

[24] F. U. Shah, O. I. Gnezdilov, R. Gusain, and A. Filippov. Transport and association of ions in lithium battery electrolytes based on glycol ether mixed with halogen-free orthoborate ionic liquid. *Scientific Reports*, 7(1):16340, 2017.

[25] D. Sinnaeve. Pfg sequence. http://DavySinnaeveet.al.

[26] Y. J. Weitsman. 2.11 - effects of fluids on polymeric compositesa review. In A. Kelly and C. Zweben, editors, *Comprehensive Composite Materials*, pages 369 – 401. Pergamon, Oxford, 2000.